LANGMUIR Article
Cite This: Langmuir 2019, 35, 3937−3948
pubs.acs.org/Langmuir

Statistical Analysis of Droplet Charge Acquired during Contact with Electrodes in Strong Electric Fields

Eric S. Elton,[†] Yash V. Tibrewala, and William D. Ristenpart*

Department of Chemical Engineering, University of California at Davis, Davis, California 95616, United States

Supporting Information

ABSTRACT: Aqueous droplets acquire charge when they contact electrodes in high-voltage electric fields. Although many researchers have investigated droplet charging under various conditions, the droplet charges are typically reported simply in terms of a mean and standard deviation. Here, we show that droplets often acquire significantly less charge for a single contact compared to the previous and subsequent contacts. These "low-charge events," which are not observed with charging of metal balls, yield up to a 60% decrease in charge acquired by the droplet and occur regardless of the applied field strength, droplet conductivity, or droplet volume. In all cases examined here, the occurrence of low-charge events to good approximation follows a negative binomial distribution (i.e., a Pascal distribution) with a mean probability of 13%. We further demonstrate that approximately 16% of charging events are characterized by "irregular" Taylor cone dynamics, suggesting that instabilities in the electrically driven deformation of the approaching liquid interface may be responsible for the low-charge events. The results indicate that workers using systems involving droplet charging should take into account the high likelihood of droplets randomly acquiring less charge than expected.

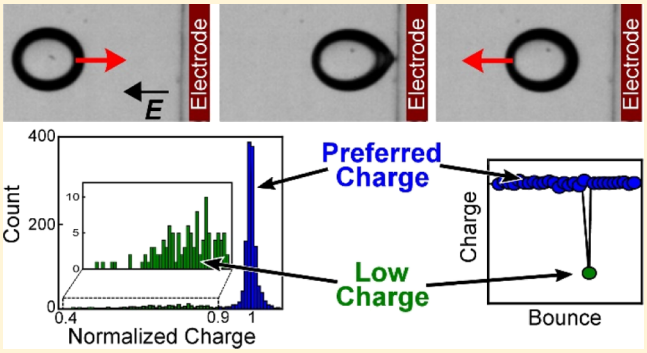

INTRODUCTION

Charged droplets are important in a variety of industrial and research applications. For example, electrostatic dehydrators use electric fields to charge and mobilize droplets so that they coalesce and sediment faster in oils and other liquids.[1,2] Electric fields are also used to control droplet motion and formation in other devices such as inkjet printers,[3] electrowetting devices,[4] and microfluidic devices,[5−9] where the electric fields have been used to induce droplet coalescence at a T-junction,[5] move droplets across streamlines,[10,11] or move droplets faster than the surrounding flow.[12−14] Electric fields have likewise been used to control droplets in a variety of other applications including droplet formation,[7,15] cell electroporation,[16,17] surface dewetting,[18] emulsion stability,[19] increased mixing,[20,21] and solute delivery for biological and chemical applications.[22]

To accurately control droplet motion, it is necessary to accurately predict and measure the amount of charge droplets acquire. A limiting prediction for the amount of charge a droplet should acquire upon contact with an electrode was derived by James Maxwell,[23] who showed that the amount of charge Q a perfectly conducting sphere would acquire from a perfectly conducting planar electrode is given by

$$Q = \frac{2}{3}\pi^3 \varepsilon\varepsilon_o a^2 E \quad (1)$$

Here, a is the sphere radius, $\varepsilon\varepsilon_o$ is the permittivity of the surrounding liquid, and E is the applied electric field. Although the amount of charge the liquid droplets acquire generally follows this dependence on electric field strength and droplet radius,[24−26] for unclear reasons droplets have not been observed to acquire as much charge as predicted by Maxwell.[7−9,22,24−30] Solid particles have also been observed to obtain less than the predicted amount of charge, again for unclear reasons.[21,27,31−36]

Although predicting the amount of charge a droplet acquires during a single contact is of fundamental interest, many applications require multiple droplet contacts, either through a single droplet contacting an electrode many times[7,12,17,22] or through multiple droplets contacting an electrode a single time.[1,3,9,15,37] Thus, in addition to being able to measure and predict the amount of charge a droplet will acquire during a single contact, it is also important to measure and predict the reproducibility of the amount of charge a droplet acquires.

Despite the large number of reports on the charging of droplets in electric fields, to date, none report statistics beyond the average and standard deviation in the amount of charge acquired. For example, Jung et al.[28] reported on the deformation and charge acquired by droplets as they contacted

Received: December 21, 2018
Revised: February 7, 2019
Published: February 13, 2019

DOI: 10.1021/acs.langmuir.8b04254
Langmuir 2019, 35, 3937−3948

electrodes, but only reported the average charge acquired over an unspecified number of contacts. Jalaal et al.[29] also reported on the deformation of droplets contacting electrodes and observed variations up to 7% in the velocity of the droplets (indicating a 7% variation in the corresponding charge). Ahn et al.[38] examined the effect of electrode geometry on the charge acquired and reported standard deviations of the charge acquired as large as 60%. Im et al.[26] observed changes in the charge acquired by different conductivity droplets under electric field strengths and observed standard deviations between 0.6 and 30%, while Elton et al.[30] observed that larger droplets (mm scale) over a wide range of conductivities had standard deviations between 8 and 26%. Eow and Ghadiri[39] and more recently Yang and Im[40] investigated the difference in charge acquired by the same droplet at different polarity electrodes. Eow reported standard deviations of 5% in the charge acquired at each electrode, while Yang reported standard deviations of 0.5% in the amount of charge acquired. Berának et al.[8] measured the frequency at which droplets transited between electrodes in a microfluidic channel and reported variations up to 10%. Finally, Elton et al.[27] observed physical cratering and other changes to the electrode caused by dielectric breakdown during charge transfer, but they only reported crater morphologies versus the average amount of charge acquired by the droplets.

Importantly, none of the above work reported statistical details beyond a mean and/or standard deviation of the amount of charge acquired by the droplets. Little is known about the underlying statistical distribution of charges acquired for multiple charging events or how the recently reported crater formation process affects the distribution.

In this work, we present a contact-by-contact analysis of aqueous droplet charge for droplets of different volumes and conductivities as they move, or "bounce," between electrodes in silicone oil. Although all of the droplets are observed to generally acquire similar amounts of charge from bounce to bounce, we demonstrate that the droplets occasionally acquire significantly less charge than previous or subsequent bounces. These "low-charge events" are ubiquitous across droplets of all conductivities and volumes studied and comprise as large as a 60% decrease in the amount of charge typically acquired by the droplet. The occurrence of low-charge events was observed to follow a Pascal distribution (i.e., a negative binomial distribution) to good approximation. In contrast, we did not observe low-charge events during the charging of metal balls. The high-speed and high-magnification video reveals that the leading edge of the droplet, which typically deforms as a classic Taylor cone,[41] instead occasionally deforms to one of a variety of different irregular shapes. This observation suggests that low-charge events are caused by less efficient charging during irregular deformation dynamics. We use these observations to offer some practical guidance for device development, as well as advice on reporting droplet charge in future investigations to account for the distinct statistical distribution of droplet charging events.

EXPERIMENTAL METHODS

The experimental setup (Figure 1, top) is similar to those used in previous experiments.[24,27,30] Standard photolithography techniques were used to deposit gold electrodes 1 mm wide, 20 mm long, and 50 nm thick onto glass substrates. For each experiment, two new electrodes were placed in a plastic cuvette and separated by nonconducting spacers at the top and bottom. One electrode was

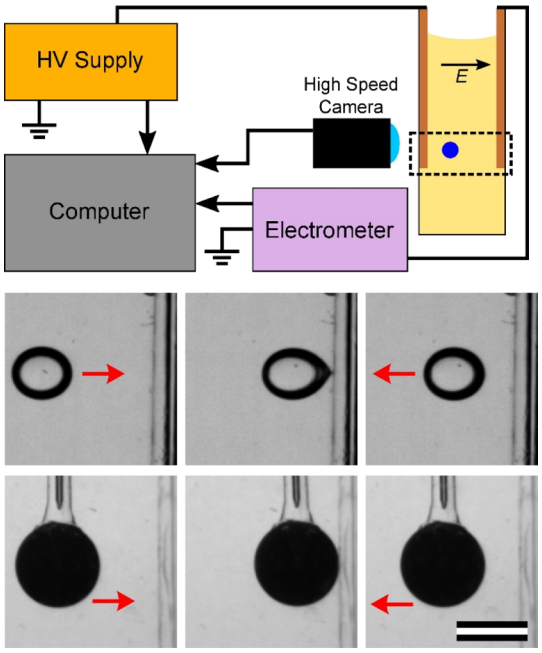

Figure 1. Top, schematic of the experimental setup. Bottom, images from a high-speed video of a 2 μL droplet (top row) or a 2.4 mm metal ball (bottom row) approaching, contacting, and departing an electrode in a 0.38 and 0.63 kV/mm electric field, respectively. Arrows indicate the direction of motion of the droplet or ball. The images are separated by 62 ms in time. The scale bar is 2 mm for all images. Also, see supporting Movies S1 and S2.

connected to a high-voltage power supply (Trek 610E), while the other was grounded through an electrometer (Keithley 6514). The cuvette was filled with 100 cSt silicone oil. Immediately prior to droplet insertion, a ZeroStat 3 antistatic gun was used to dissipate any static charge on the cuvette surface.

For each experiment, an aqueous droplet of specified volume (0.5−3.5 μL) and conductivity (0.001−113 mS/cm) was manually pipetted between the electrodes. Droplet conductivity was controlled by the addition of potassium chloride (Sigma-Aldrich reagent grade) in different concentrations to deionized water. The conductivity of the bulk solution was measured immediately prior to each experiment. Upon insertion into oil, the droplet was initially attracted to one electrode where it made a contact, received a charge, and was repelled toward the other electrode, whereupon the process repeated (Figure 1, middle and Movie S1). Owing to the larger density of the droplet compared to the silicone oil, droplets sank downward. As the droplets approached the bottom of the electrodes, positive dielectrophoretic forces[42] counteracted gravity and caused them to bounce at approximately the same vertical location for the remainder of the experiment.

A high-speed video of the droplet was recorded using a Phantom v7.3 camera at 500 images per second, while the analog signal from the electrometer was recorded using a digital acquisition card at a rate of 50 kHz. Care was taken to allow the droplet to completely settle near the bottom of the electrodes before recording the high-speed video used to determine the droplet charge. At the end of each experiment, the droplet was removed from the experimental cell prior to deactivating the applied voltage. Depending on the applied voltage and droplet volume, between approximately 50 and 200, successive bounces were recorded per experiment.

The charge acquired by the droplet was determined using a standard force-balance technique.[24−28,30−32,40,43−45] In brief, during moments of constant velocity (near the midplane of the cuvette), the drag force ($F_D = 4\pi\lambda\mu aU$) on the droplet was balanced with the electrostatic force ($F_E = QE$). The resulting charge is given by $Q = 4\pi\lambda\mu aU/E$, where μ is the viscosity of the oil, a is the droplet radius,

DOI: 10.1021/acs.langmuir.8b04254
Langmuir 2019, 35, 3937−3948

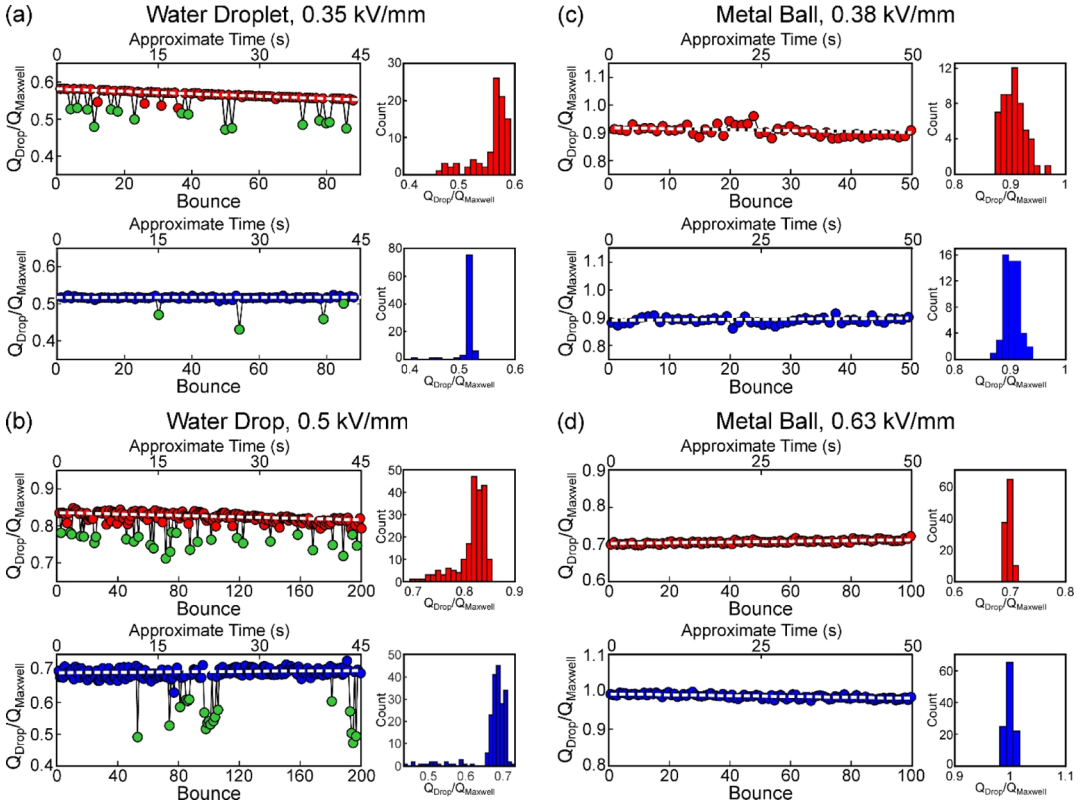

Figure 2. Representative examples of charges acquired during successive charge transfer events by a water droplet or a metal pendulum. (a,b) Positive (red) and negative (blue) charges acquired during each contact by 2 μL deionized water droplets in a 0.35 and 0.5 kV/mm electric field, respectively. (c,d) Positive (red) and negative (blue) charges acquired during each contact by a 2.4 mm diameter metal ball bouncing in a 0.38 and 0.63 kV/mm electric field, respectively. Histograms of the charge distribution are to the right of each plot. The secondary axis on each plot gives the approximate time progression during the experiment, as estimated from the total time the droplet or ball took to complete the total number of bounces displayed. The dashed line is the "preferred charge" as determined through linear regression. All charges are normalized by the Maxwell charge given in eq 1. Note that there are many low-charge events for the water droplet, but none for the metal ball.

and U is the droplet velocity. The Hadamard−Rybinzsky correction factor, λ, is 1 because the viscosity of oil is much greater than that of the aqueous droplet (i.e., $\mu_{oil} \gg \mu_{drop}$).[46,47] The electric field is estimated as $E = V/H$, where V is the applied voltage and H is the distance between the electrodes. The droplet velocity and radius were determined by processing the recorded high-speed video and detecting the droplet centroid and projected area using standard image analysis algorithms in MatLab.

The force-balance technique was not used to determine the charge acquired by solid particles because the drag force on the pendulum support was not known a priori. Instead, the charge acquired by the aluminum ball was determined via a nonlinear regression of a model of the system current to the observed current using a methodology described previously.[24] We focus here primarily on variations of the observed charge acquired by droplets and particles through successive charge transfer events (i.e., "bounces").

RESULTS

Representative experimental measurements of two individual water droplets and two individual metal balls bouncing between electrodes in different electric field strengths are shown in Figure 2. The charge acquired by both aqueous droplets and metal balls is strongly dependent on the magnitude of the electric field, and therefore, the charge data in Figure 2 have been normalized by the Maxwell charge given in eq 1 to facilitate comparison of different experiments. Droplets most often received a similar charge as the previous and subsequent bounces, with this charge value denoted here as the "preferred charge" of the droplet (indicated by the dashed white lines, cf. discussion of the regression scheme below). However, significant decreases from the preferred charge are frequently observed during the charging of water droplets (the green data points in Figure 2). These "low-charge events" occurred most commonly as single bounces (cf. Figure 2a), but also occasionally as two or more subsequent bounces (cf. Figure 2b, negative charge).

In contrast to aqueous droplets, no low-charge events were observed during the charging of metal balls (Figure 2c,d). Instead, the charge acquired by solid particles was always close to the preferred charge (i.e., the charge acquired by the ball was always observed to be similar from bounce to bounce). This behavior is most apparent in histograms of the charge acquired by the droplet or ball (Figure 2). Both of the metal ball histograms demonstrate a narrow distribution of charges around the preferred charge. The histograms of the droplet charge, however, also exhibit a long left-hand tail caused by the low-charge events. This long tail is absent in the histograms of the charge acquired by the metal ball. The charge acquired by the metal ball was also more tightly grouped around the median than that acquired by the droplet. On average, 98% of metal ball bounces yielded charges within 5% of the median amount of charge acquired, while only 85% of droplet bounces yielded charges within 10% of the median amount of charge acquired. Droplets rarely acquired a charge significantly more than the preferred charge.

DOI: 10.1021/acs.langmuir.8b04254
Langmuir 2019, 35, 3937−3948

A key observation is that the preferred charge may increase or decrease slightly with time. The representative droplet in Figure 2a exhibited a slight downward trend in charge as time progressed, whereas the droplet in Figure 2b maintained a more constant charge with time. Droplets generally acquired less charge as time progressed (Figure S1). The positive charge acquired by the droplets on average decreased by 2.5% in 30 s, although the magnitude of the change in charge acquired by the droplet varied between −6 and +3%. Similarly, the magnitude of the negative charge acquired by the droplets decreased by 0.8% in 30 s on average, although the amount of change in charge acquired by the droplet ranged between −5 and +4%.

Determination of Low-Charge Events. The representative data in Figure 2 indicate that despite the existence of a preferred charge, droplets occasionally acquire significantly less charge than previous or subsequent bounces (i.e., "low-charge events"). To more rigorously define low-charge events, a two-step process was utilized during which the ostensible preferred charge was first identified by linear regression, and the low-charge events were then identified as charges that were deemed sufficiently small compared to the preferred charge.

Because the preferred charge depended sensitively on the applied voltage and droplet volume, we identified it for each experiment via linear regression of the observed charges for that particular experiment. Inclusion of all the charge data in the linear regression often gave very poor fits because a single low-charge event can dramatically impact the slope of the best-fit line. To limit the effect of low-charge events on the slope of the regression line, only charge data which fell in the range

$$Q_{50} - (Q_{75} - Q_{50}) \leq Q \leq Q_{75} \tag{2}$$

were used to find the preferred charge, where Q_{50} is the median, or 50th percentile, of all charges acquired by the droplet and Q_{75} is the 75th percentile of the charges acquired. This procedure eliminated the highest and lowest charges while preserving enough data points for a linear fit, independent of the number and magnitude of any low-charge events (cf. dashed white lines in Figure 2).

Low-charge events were then found by assessing the absolute difference D of the observed charge from the best-fit preferred charge line. Low-charge events were defined as charges which were removed from the best-fit line by more than twice the median absolute deviation (MAD) of differences of all charges from the preferred charge, that is, charges with an absolute difference

$$D > D_{50} + 2\mathrm{MAD}(D) \tag{3}$$

where D_{50} is the median of all absolute differences. The median and MAD were used to find low-charge events because they are more robust than the mean and standard deviation when significant numbers of outliers exist.[48]

Factors Affecting the Occurrence of Low-Charge Events. The low-charge events present during the charging of water droplets and the lack of low-charge events during the charging of metal balls are both readily seen in histograms of the amount of charge acquired by the droplet or ball. Figure 3 presents a histogram of charges acquired by droplets and balls compiled from several different experiments at different applied voltages. Because the charge acquired by the droplet depends on the applied voltage, the charge data for each experiment were normalized by the median amount of charge acquired by the droplet or ball in that particular experiment, and all charge data are presented in a single histogram. The histograms of charges acquired by droplets clearly show a long left-hand tail at lower charges, while the histograms of charges acquired by solid balls are normally distributed around the median.

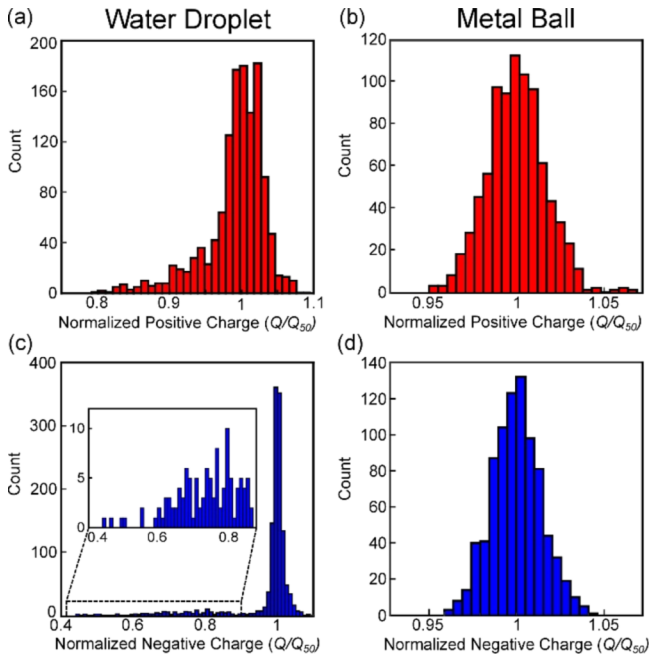

Figure 3. Histograms of the amount of charge acquired by 2 μL deionized water droplets (a,c) and 2.4 mm metal balls (b,d). Each histogram is compiled from several different experiments at different applied voltages. To compare the different experiments, the charges from each experiment were normalized by the median of the charge acquired during each experiment. The inset in (c) shows the distribution of normalized charges from 0.4 to 0.9. Water droplet histograms represent 1290 bounces from 8 different experiments. Metal ball histograms represent 840 bounces from 4 different experiments. Note the lower charge (left hand) tail present in the histograms of charge acquired by water droplets.

To test whether applied voltage affected the propensity for low-charge events to occur, the same charge data aggregated in Figure 3 are presented in boxplots in Figure 4 as a function of the applied voltage. Each circle in Figure 4 represents an individual bounce, while the blue box bounds the 75th and 25th percentiles of all bounces. The red line is the median of all charges acquired by the droplet or ball. The charges have been normalized by the Maxwell charge (eq 1) to facilitate comparison of data at different electric field strengths. Both the positive and negative charges acquired by droplets grow closer to the limiting Maxwell charge as the electric field is increased, although droplets were never observed to fully acquire the Maxwell charge. Metal balls always acquired similar amounts of charge relative to the Maxwell charge, regardless of the applied electric field. Low-charge events, denoted by green circles, are observed for all 2 μL deionized water droplets bounced in electric fields between 0.35 and 0.52 kV/mm. No low-charge events (as defined by eq 3) are observed during the charging of solid metal balls bouncing in electric fields between 0.375 and 1.13 kV/mm.

The effect of droplet conductivity and droplet volume on the occurrence of low-charge events was also investigated. Figure 5 shows the amount of charge acquired by droplets of different

DOI: 10.1021/acs.langmuir.8b04254
Langmuir 2019, 35, 3937−3948

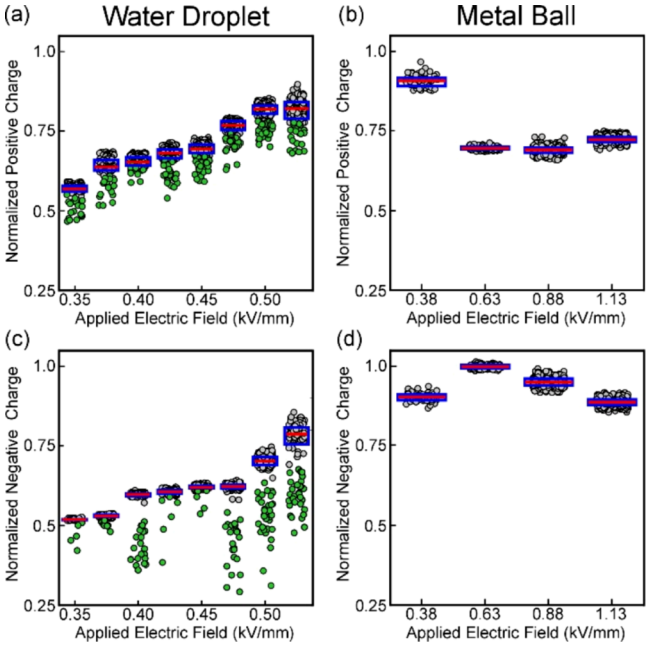

Figure 4. Comparison of charges acquired by water droplets vs metal balls. (a,b) Positive charge acquired by 2 μL deionized water droplets (a) and 2.4 mm diameter metal balls (b) bouncing between electrodes in different electric field strengths. (c,d) Negative charge acquired by deionized water droplets (c) and metal balls (d) bouncing between electrodes in different electric field strengths. In all plots, observed charges have been normalized by the Maxwell charge given in eq 1. For clarity, each data point is randomly distributed from the center of the column. The blue box indicates the 25th and 75th percentiles. The red line is the median of the data. Green points are low-charge events.

conductivities. Each boxplot in Figure 5 represents an individual experimental trial, with a unique droplet and set of electrodes. Droplets of all conductivities acquired similar amounts of charge (i.e., the variation between individual experiments at any specific conductivity was greater than any other noticeable trend). The cause of the variations in mean droplet charge between experiments is not currently known; despite our best efforts to minimize such effects, possible explanations include changes to the electric field caused by electrode alignment or changes to the drag experienced by the droplet due to contamination. Droplets of all conductivities also experienced low-charge events on both positive and negative electrodes.

Figure 6 shows the effect of droplet volume on low-charge events. Droplets of different volumes experienced low-charge events at both the positive and negative electrodes. Droplets of different volumes also acquired similar amounts of charge relative to the limiting Maxwell charge, consistent with previous results indicating that the amount of charge increases with the square of the radius of the droplet.[25,26]

A final observation is that the magnitude of low-charge events varied between positive and negative electrodes. On average, low-charge events resulted in a 9% decrease in charge relative to the preferred charge at the positive electrode and a 29% decrease in charge at the negative electrode (Figure S2). The larger difference in the charge magnitude at the negative electrode was present for all droplets, regardless of the droplet volume, the droplet conductivity, or the applied voltage. Although it is unclear why low-charge events were more dramatic at the negative electrode, we note that droplets always received less charge at the negative electrode than the positive electrode. The larger decrease in charge at the negative electrode may be related to the lower amount of charge passed to the droplet overall.

Statistical Model for Low-Charge Events. The percentage of low-charge events, as defined by eq 3, out of all bounces in each experimental trial ranged from 3 to 29% for all trials (Figure 7). There was little difference in the percentage of low-charge events that occurred at positive or negative electrodes (Figure 7a). The median of the percentage of low-charge events per trial was 12.4% for the positive electrode and 13.7% for the negative electrode. The Wilcoxon rank sum test returns a p value of 0.86, indicating that it is unlikely the positive and negative charge data derived from distributions with the different median values. Thus, for any given bounce, a droplet has a 13% chance of acquiring a low charge from either electrode. No clear trends in the percentage of low-charge events were detected, as the applied voltage, droplet conductivity, or droplet volume was varied (Figure 7b–d).

The autocorrelation of the occurrence of low-charge events is shown in Figure 8. The autocorrelation was calculated using a binary vector where 0 represented the normal charge events and 1 represented the low-charge events. The red lines in

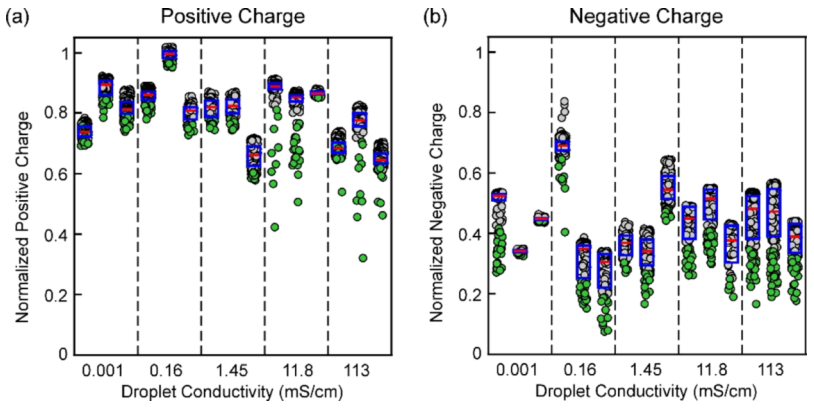

Figure 5. Positive (a) and negative (b) charges acquired by 3.5 μL water droplets of different conductivities bouncing between electrodes in a 0.41 kV/mm applied electric field. Observed charges have been normalized by the Maxwell charge given by eq 1. For clarity, each data point is randomly distributed from the center of the column. The blue box indicates the 25th and 75th percentiles. The red line is the median of the data. Green points are low-charge events.

DOI: 10.1021/acs.langmuir.8b04254
Langmuir 2019, 35, 3937–3948

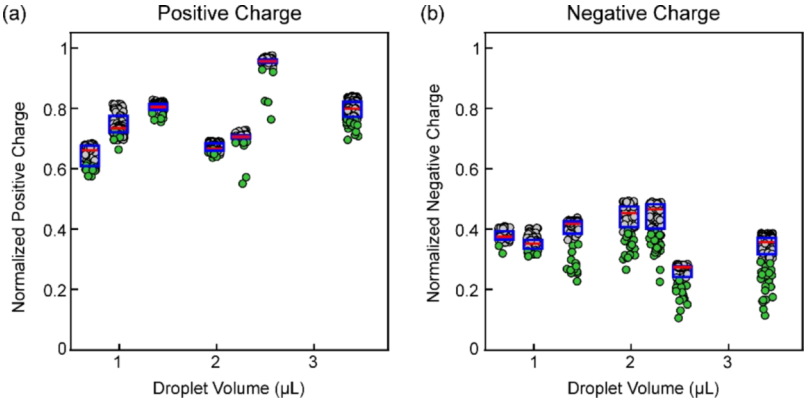

Figure 6. Positive (a) and negative (b) charges acquired by different volume 0.1 M KCl droplets bouncing between electrodes in a 0.41 kV/mm applied electric field. Observed charges have been normalized by the Maxwell charge given by eq 1. For clarity, each data point is randomly distributed from the center of the column. The blue box indicates the 25th and 75th percentiles. The red line is the median of the data. Green points are low-charge events.

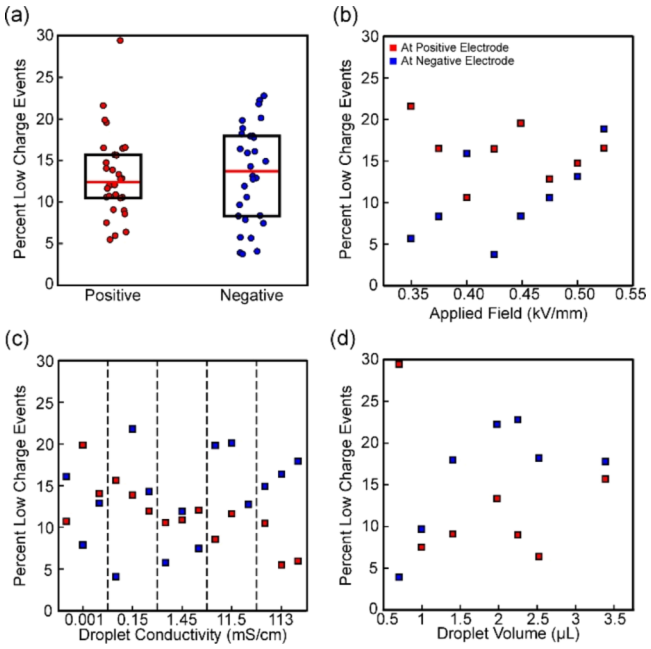

Figure 7. (a) Percentage of low-charge events which occurred for each experimental trial at positive and negative electrodes. Individual data points represent individual experimental trials. The black box bounds the 75th and 25th percentiles. The red line is the median of the data. For clarity, the data points are horizontally offset randomly from the middle of the column. (b–d) Percentage of low-charge events which occur for (b) 2 μL droplets bouncing in different applied fields, (c) 3.5 μL droplets of different conductivities bouncing in a 0.4 kV/mm field, and (d) different volume deionized water droplets bouncing in a 0.4 kV/mm field. Red data points are from the positive electrode, and blue points are from the negative electrode.

Figure 8 indicate the limits of statistical significance, at a 95% confidence interval, as calculated by $p = \pm 1.96/\sqrt{N}$, where N = 8378 is the total number of charge events examined.[49] The only statistically significant autocorrelation occurs at low lag numbers and is extremely weak (i.e., ACF < 0.08). This low value indicates that the occurrence of a low-charge event had virtually no influence on the probability of another low-charge event occurring during a subsequent contact.

Despite the seemingly random distribution of low-charge events, their occurrence appears to follow a negative binomial

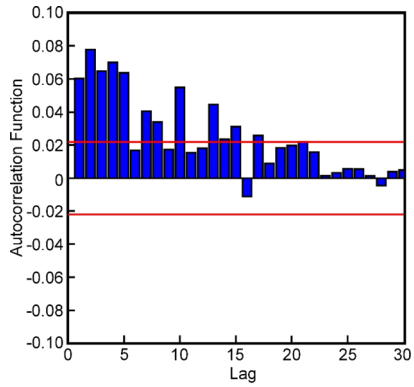

Figure 8. Autocorrelation function of the occurrence of low-charge events. The lag is the difference between bounces. Red lines indicate the 95% confidence interval. Note that the autocorrelation is extremely weak (<0.08) for all values of the lag.

distribution. Also known as a Pascal distribution, the negative binomial distribution is appropriate for over-dispersed count data for which the Poisson distribution is not appropriate[50−52] and is used to model infrequent random events such as the length of hospital stays[53] or traffic accident frequency.[54] The Pascal distribution describes the probability of a certain number of successes before a certain number of failures occur or, in this case, the number of preferred charge events before a given number of low-charge events. Figure 9a shows the probability of a certain number of bounces occurring before a single low-charge event occurs. The solid markers are experimental data, while the open markers are a Pascal distribution with a probability of a low-charge event per bounce of 0.13. The distribution qualitatively accords with the experimental data. The Pascal distribution also fits for higher numbers of low-charge events, such as 2 or 5 (Figure 9b,c). The qualitatively good fit of the Pascal distribution to the experimental data suggests that low-charge events are caused by a randomly recurring process.

Deformation Dynamics of Droplets Approaching Electrodes. To summarize, all droplets observed experienced low-charge events, regardless of the applied voltage, droplet volume, or droplet conductivity. In contrast, no low-charge events occurred during charge transfer to metal balls. A key question, then, is why do droplets experience low-charge events while metal balls do not? One key difference between

DOI: 10.1021/acs.langmuir.8b04254
Langmuir 2019, 35, 3937−3948

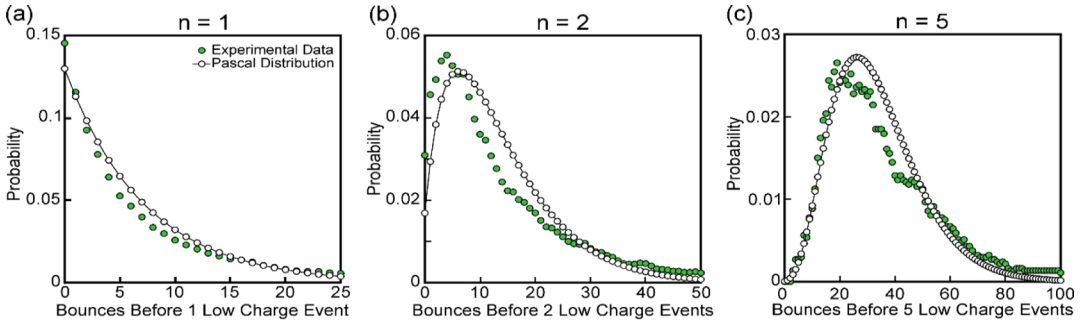

Figure 9. Probability of a low-charge event follows the Pascal distribution. The probability of a certain number of bounces before the first (a), second (b), or fifth (c) low-charge event occurs. Green data points are experimental data. The open data points are a Pascal distribution with a probability of a low-charge event per bounce of 0.13. Solid lines are guides for the eye.

liquid droplets and metal balls is that droplets deform as they approach and contact the electrode (cf. Figure 1). We hypothesized that the deformation of the water droplet as it approaches the electrode is responsible for the observed low-charge events.

To test the hypothesis that droplet deformation is at least partially responsible for low-charge events, we observed the moment of contact between droplets and electrodes via high-speed video. Using high optical magnification and frame rates between 12 000 and 24 000 frames/s, six unique types of contact dynamics between droplets and electrodes were observed (Figure 10 and supporting Movies S3–S8). The droplet was most often observed to deform into a single axisymmetric cone that subsequently came into apparent contact with the electrode (supporting Movie S3). This Taylor cone[41,55] behavior has been widely observed before[24−30] and is because of the competition of the droplet surface tension and applied electrical stress.

Although axisymmetric single cones were observed most frequently, droplets were also observed to occasionally deform into other less regular shapes. Among the "irregular" contact dynamics observed, droplets deforming to form two concurrent Taylor cones were most common (supporting Movie S4). Although droplets have been observed to form Taylor cones on opposing poles,[41] it is unclear why two Taylor cones would form on the same side of the droplet. Multiple Taylor cones and jets have been observed to form when fluid flowing out of a capillary is injected with charge via a submerged electrode.[56−58] The multiple cones and jets form to release the increased amount of charge more efficiently. Thus, it is possible that the droplet deforms to a double cone to spread out a high surface charge concentration.

Droplets were also observed to contact the electrode via a single Taylor cone that extended asymmetrically from the droplet (i.e., the center of mass of the droplet was not aligned with the center of the Taylor cone). These droplets were often close to the end of the electrode, and the cone appears to extend from the portion of the droplet closest to the electrode (supporting Movie S5). This behavior suggests that the cone was extending in the direction of the strongest electric field, as would be expected.

Another contact dynamic observed involved droplets expelling a liquid jet just prior to contacting the electrode (supporting Movie S6). Charged droplets are known to expel charged jets when the surface charge exceeds the Rayleigh stability criterion.[41,55,59] The formation of jets may be due to the surface charge of the droplet locally exceeding the Rayleigh stability limit, although the total droplet charge remains below the limit.

Occasionally, droplets were observed to contact sessile drops that were presumably left on the surface of the electrode by previous droplet contacts (supporting Movie S7). It is unclear why droplets left behind small sessile drops on the electrode surface, although variations in the electrode surface either caused by previous droplet bounces or photolithography defects may have created local changes in the wettability of the electrode surface. Once a drop was deposited on the surface of the electrode, incoming charged droplets could be drawn toward the increased electric field caused by the raised sessile drop and make a preferential contact with the sessile drop rather than the electrode.

Finally, more complex dynamics, such as droplets forming a double Taylor cone and simultaneously extending a liquid jet, were also observed (Movie S8). It is unclear why these complex dynamics occur; it is possible that the same underlying causes for the other irregular dynamics occur in tandem to cause the combined complex dynamics.

Importantly, the same droplet was observed to contact the electrode in different ways during subsequent bounces. The droplet always appeared to make a physical contact with the electrode during each bounce, at least to the resolution possible with the high-speed video. Previous work has indicated that dielectric breakdown, as evidenced by a flash of light detected by a photomultiplier tube, can occur between the droplet and the electrode during charge transfer.[27,30] It has been hypothesized that the charging of droplets and other particles via dielectric breakdown resulted in very small gaps (~100 nm) between the droplet and electrode instead of a physical contact.[35,36] The resolution of the images acquired here is not sufficient to discern such small gaps, and the droplet appears to make a physical contact with the electrode during each bounce.

Figure 11 shows the percentage of observed bounces which resulted in each of the observed contact dynamics. Droplets were observed to contact the electrode via a single Taylor cone approximately 84% of the time. The second most common contact dynamic was the double cone, which was observed in approximately 7% of all bounces. The other irregular behaviors occurred in about 1−3% of all bounces. Notably, all of the irregular contact dynamics combined accounted for approximately 16% of the observed bounces, which is close to the observed frequency of low-charge events (13%). This observation implies that the droplet acquires the preferred

DOI: 10.1021/acs.langmuir.8b04254
Langmuir 2019, 35, 3937−3948

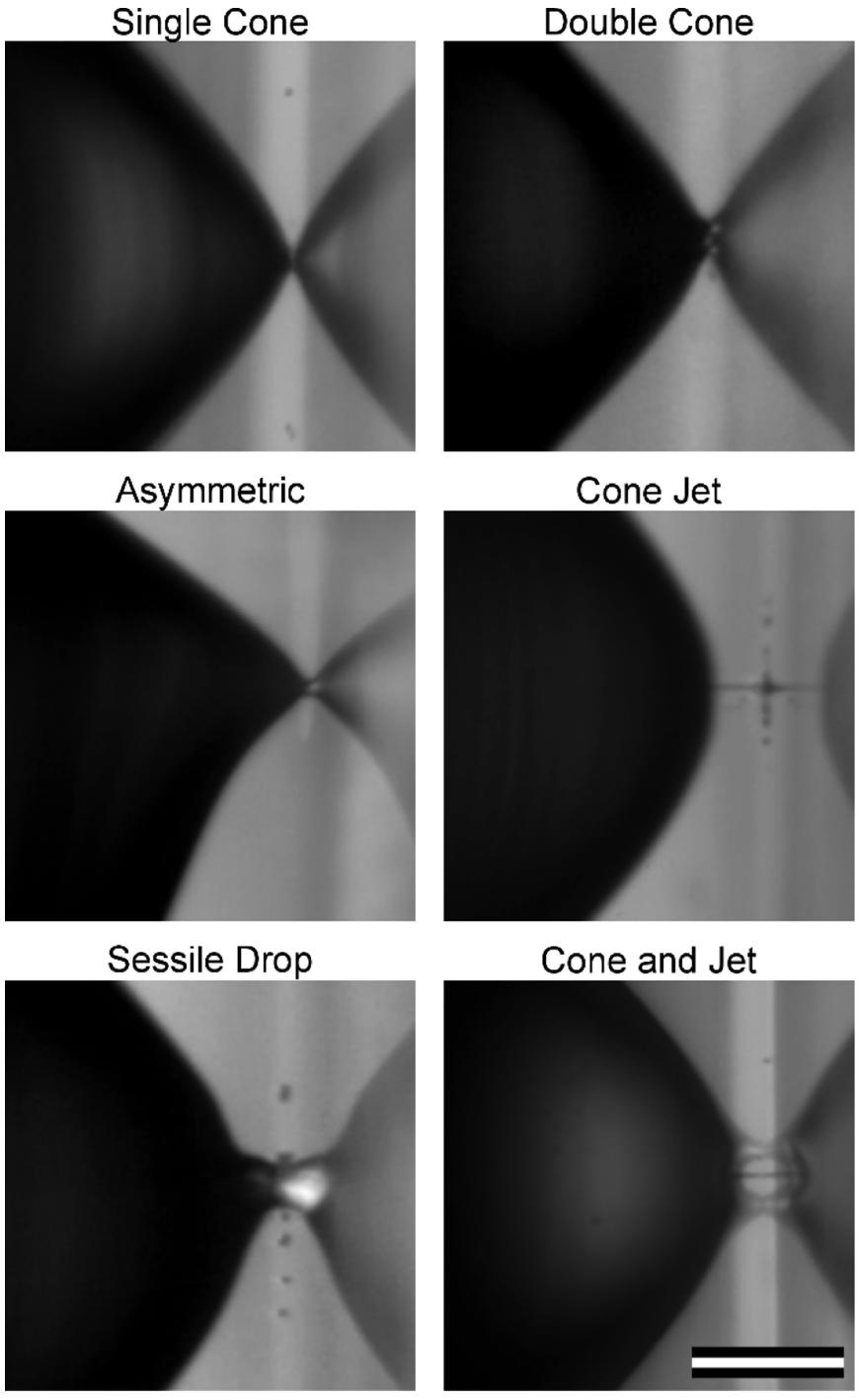

Figure 10. Varying dynamics of the droplet contact with electrodes. The scale bar is 150 μm for all pictures. Also, see supporting Movies S3–S8.

charge when contacting via a single cone and acquires a low charge when contacting via any other method.

We were not able to directly estimate the amount of charge the droplet acquired during each contact because the high magnification used to visualize droplet contact did not allow us to visualize the entire droplet transit or make any reasonable estimate of the droplet velocity. We attempted to align the recorded video and recorded current trace to estimate the charge acquired by the droplet via the recorded current, but the high magnification of the video blocked the view of the overall trajectory of the droplet and complicated the alignment of the recorded current and video data with confidence. Nonetheless, the similar percentages of low-charge events and irregular droplet contacts strongly suggest that droplets acquire the preferred charge when contacting via a single cone and a low charge when contacting via any other dynamic.

DISCUSSION

The overarching conclusion of this work is that aqueous droplets randomly obtain much lower amounts of charge than average, regardless of voltage, conductivity, or volume. The frequency of these low-charge events is described by the Pascal distribution with a mean probability of 13%. In contrast, metal balls bouncing between electrodes were not observed to

DOI: 10.1021/acs.langmuir.8b04254
Langmuir 2019, 35, 3937–3948

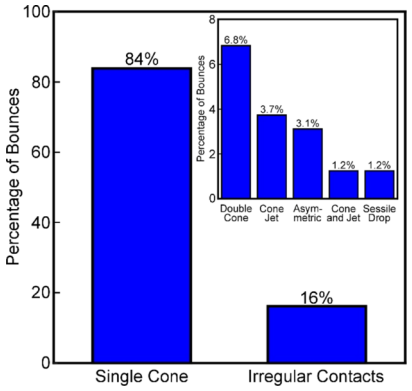

Figure 11. Frequency of observed contact dynamics of 3.5 μL droplets. The inset shows the frequency of all "irregular" contact dynamics besides single cone. The sample size is 161 individual droplet contacts from 8 different experiments.

experience low-charge events, suggesting that low-charge events are unique to the charge transfer between liquid droplets and electrodes, and not a general consequence of repeated charge transfer between conducting objects.

Importantly, the occurrence rate of low-charge events (13%) is commensurate with the occurrence rate of irregular droplet deformation dynamics (16%). This observation raises the question: Why would the method of contact affect the amount of charge the droplet acquires? The exact mechanism of the charge transfer between electrodes and droplets is not well understood,[17,30] making it difficult to say exactly how the different contact dynamics affect charge transfer. Previous researchers have speculated that electrochemical reactions involving the droplet and electrode metal are responsible for the charge transferred.[8,17,28] Thus, the different contact dynamics may cause a decrease in the effective contact area or time, which could affect the extent of any electrochemical reactions. More recently, Elton et al. have observed dielectric breakdown occurring between sufficiently high-conductivity droplets and electrodes during charge transfer.[27,30] As droplets approached the electrode, the electric field between the droplet and electrode overcame the dielectric breakdown strength of the insulating fluid, causing an arcing event. The local electric field between the droplet and electrode is sensitive to the curvature of the droplet; therefore, a droplet deforming in an irregular dynamic may not experience dielectric breakdown prior to a direct electrode contact, which might alter the amount of charge transferred to the droplet.

In some cases, it is easy to envision why the droplet could acquire lower charge as a consequence of some irregular contact dynamics. For example, a droplet which ejects a highly charged cone jet just prior to contacting the electrode could acquire much less charge because jets emitted from charged droplets are known to be highly charged,[41,60,61] and accordingly, some of the charge is transferred via the jet instead of via a direct contact. Similarly, a droplet contacting a sessile drop already on the electrode must exchange charge with the electrode through the sessile drop, a process which may be limited either by the droplet conductivity or sessile drop size,[43] rather than the electrical properties of the electrode.

It is more difficult to envision why other contact dynamics could lead to lower amounts of charge acquired by the droplet. It is important to remember that droplets deform to balance electrical and surface tension forces,[41,55] so a droplet deforming to form double Taylor cones, or any of the other observed irregular contact dynamics, is presumably responding to a different electric field than a droplet which deforms into a single Taylor cone. Because droplets acquire different amounts of charge depending on the electric field,[24−26] a change in the local electric field may directly affect the amount of charge droplets acquire.

One clear example of the local electric field affecting the droplet deformation is droplets that contact the electrode in an asymmetric manner. These droplets were observed to be very close to the bottom end of the electrode, and it is likely that these droplets experienced a lower electric field strength than droplets which contacted the electrode higher where the electric field is more uniform. The decrease in the electric field strength could lead to their lower charge acquired. It is unclear why droplets would sink slightly downward toward the bottom of the electrode and then rise again in subsequent bounces.

Except for changes in the droplet location relative to the electrode, it is not clear why the droplet would experience a different electric field on subsequent bounces. One possibility is that the electrode was physically changed during the previous charge transfer events. Electrode deformations that could cause variations in the local electric field, including bumps and craters, were observed to be caused by heat released from dielectric breakdown between droplets and electrodes during charge transfer.[27,30] Only high-conductivity droplets caused cratering on the electrode, however, so the observation that low-conductivity deionized water droplets also often experienced low-charge events indicates that electrode cratering cannot be the only reason for the low-charge events to occur.

The electric field between the droplet and electrode is also affected by the charge density of the incoming droplet because the droplet charge will affect the potential difference between the droplet and electrode. We do not observe any clear correlation between droplet charges prior to bounces where the droplets acquire the preferred charge or a low-charge event (Figure S3), suggesting that the charge of the incoming droplet by itself is not responsible for low-charge events.

A final possibility is that the charges on the droplet surface are unable to move fast enough to rearrange evenly as the droplet approaches the electrode, resulting in a different local electric field between the electrode and droplet. The charge relaxation time, or the characteristic time for charges to rearrange on the surface of the droplet, is 7 μs for deionized water droplets, which is much faster than the observed contact dynamics (~83 μs, or one frame, in the high-speed video). The fast charge relaxation time relative to contact time suggests that charges have sufficient time to rearrange as the droplet deforms prior to contacting the electrode, and thus, the exact charge arrangement is unlikely to be responsible for low-charge events.

Regardless of why droplets experience low-charge events, their occurrence may have a significant impact on the reported average and standard deviation of reported charge values. Many literature reports provide just an average and standard deviation of the charge transferred to the droplet. The presence of a single low-charge event during an experiment may significantly change the average and standard deviation of the recorded data, invalidating the assumption that the standard deviation is an accurate representation of the charge variation. In some cases, reporting the median of the charge

DOI: 10.1021/acs.langmuir.8b04254
Langmuir 2019, 35, 3937−3948

rather than the mean may give a more appropriate measure of the usual amount of charge, particularly if a small number of bounces is analyzed.

Finally, two other general observations should also be briefly discussed. First, all droplets observed acquired more positive charge than negative charge, regardless of the droplet volume, the droplet conductivity or the applied field strength. This observation is consistent with multiple previous reports (see ref 24 for a review). The cause for this imbalance is not currently well understood, although it may be because of residual static charge on the surface of the cuvette or the surface of the electrode substrate.[40] Although we took care to remove excess static charge prior to inserting the droplet, we made no attempt to measure the residual static charge on the surface of the cuvette.

Interestingly, metal balls were observed to acquire more negative charge than positive charge (cf. Figure 4), which is in contrast to several previous reports.[31−33] It remains unclear why this occurred because the experimental setup was prepared similarly for both droplet and solid particle experiments, although static charge on the glass rod support connected to the metal ball may affect the measurement of the charge on the ball.

A second general observation is that droplets were always observed to acquire less than the theoretical maximum amount of charge a spherical conductor should acquire from an infinitely planar electrode as calculated by Maxwell. This result has also been widely observed in the past[22,24−30,39,40] and may be due to the deformation of the droplet as it approaches the electrode,[22,28] the limited conductivity of the droplet,[25,26] or dielectric breakdown which occurs between the droplet and electrode as the droplet approaches.[27,30] It is unclear why metal balls also acquired less charge than predicted, although it has been suggested that dielectric breakdown between the ball and electrode may prevent actual contact from occurring, thus limiting the amount of charge the ball acquires.[35,36]

CONCLUSIONS

A bounce-by-bounce analysis of the charge acquired by aqueous droplets reveals that droplets randomly obtain much lower amounts of charge than previous or subsequent bounces, regardless of the applied voltage, droplet conductivity, or droplet volume. In contrast, metal balls were never observed to experience low-charge events, suggesting that low-charge events are unique to charge transfer between aqueous droplets and electrodes and not a consequence of repeated charge transfer between conducting objects. The frequency of low-charge events is described by a Pascal distribution with a mean probability of 13%. Importantly, the rate of occurrence of low-charge events (13%) is similar to the observed occurrence rate of irregular droplet deformation dynamics (16%), suggesting that the low-charge events are caused by irregular droplet deformation dynamics.

On a fundamental level, the results presented here indicate a need for more research in understanding the exact charge transfer process and the exact role of the electric field in determining how the droplet contacts the electrode. Perhaps more importantly, the results presented here have implications in the reporting and quantifying of the charge acquired by droplets. A single low-charge event during an experiment with a limited number of bounces may significantly change the reported average and standard deviation of the charge acquired by the droplet. In terms of practical applications, the results presented here are of fundamental interest in the development of electrocoalesers,[1,37] electrostatic dehydrators,[2] lab-on-a-chip-type devices,[7,8,22] and other devices[3,43,44,62] which use electric fields to manipulate droplets. Workers designing these systems for practical applications should be aware that droplets will frequently obtain a significantly lower charge than anticipated and design their systems accordingly.

ASSOCIATED CONTENT

Supporting Information

The Supporting Information is available free of charge on the ACS Publications website at DOI: 10.1021/acs.langmuir.8b04254.

Percent change in the magnitude of the charge acquired by droplets in 30 seconds, percent difference of charge acquired during low-charge events from the preferred droplet charge, and comparison of incoming droplet charge to the positive and negative charges acquired by the droplet (PDF)

2 μL droplet bouncing between electrodes in silicone oil (MPG)

2.4 mm ball bouncing between electrodes in silicone oil (MPG)

3 μL droplet contacting an electrode as a single cone (MPG)

3 μL droplet contacting an electrode as a double cone (MPG)

3 μL droplet contacting an electrode asymmetrically (MPG)

3 μL droplet ejecting a jet prior to contacting an electrode (MPG)

3 μL droplet contacting a sessile drop on an electrode (MPG)

3 μL droplet deforming to form two cones and emitting a single jet prior to contacting an electrode (MPG)

AUTHOR INFORMATION

Corresponding Author

*E-mail: wdristenpart@ucdavis.edu.

ORCID

William D. Ristenpart: 0000-0002-4935-6310

Present Address

†Materials Engineering Division, Lawrence Livermore National Laboratory, 7000 East Ave, Livermore, CA 94550, USA.

Notes

The authors declare no competing financial interest.

ACKNOWLEDGMENTS

We thank the UC Davis Center for Nano-Micro Manufacturing for use of their equipment in electrode fabrication. We also thank the NSF Particulate and Multiphase Processes program for support (award 1707137). Manuscript preparation was performed under the auspices of the U.S. Department of Energy by Lawrence Livermore National Laboratory under Contract DE-AC52-07NA27344. IM Release Number LLNL-JRNL-763358.

REFERENCES

(1) Eow, J. S.; Ghadiri, M.; Sharif, A. O.; Williams, T. J. Electrostatic Enhancement of Coalescence of Water Droplets in Oil: A Review of the Current Understanding. *Chem. Eng. J.* **2001**, *84*, 173−192.

DOI: 10.1021/acs.langmuir.8b04254
Langmuir 2019, 35, 3937−3948

(2) Zolfaghari, R.; Fakhru'l-Razi, A.; Abdullah, L. C.; Elnashaie, S. S. E. H.; Pendashteh, A. Demulsification Techniques of Water-in-Oil and Oil-in-Water Emulsions in Petroleum Industry. *Sep. Purif. Technol.* **2016**, *170*, 377−407.
(3) Calvert, P. Inkjet Printing for Materials and Devices. *Chem. Mater.* **2001**, *13*, 3299−3305.
(4) Mugele, F.; Baret, J.-C. Electrowetting: From Basics to Applications. *J. Phys.: Condens. Matter* **2005**, *17*, R705−R774.
(5) Link, D. R.; Grasland-Mongrain, E.; Duri, A.; Sarrazin, F.; Cheng, Z.; Cristobal, G.; Marquez, M.; Weitz, D. A. Electric Control of Droplets in Microfluidic Devices. *Angew. Chem., Int. Ed.* **2006**, *45*, 2556−2560.
(6) Baroud, C. N.; Gallaire, F.; Dangla, R. Dynamics of Microfluidic Droplets. *Lab Chip* **2010**, *10*, 2032−2045.
(7) Vobecká, L.; Khafizova, E.; Stragier, T.; Slouka, Z.; Přibyl, M. Electric Field Driven Addressing of ATPS Droplets in Microfluidic Chips. *Microfluid. Nanofluid.* **2017**, *21*, 51.
(8) Beránek, P.; Flittner, R.; Hrobař, V.; Ethgen, P.; Přibyl, M. Oscillatory Motion of Water Droplets in Kerosene above Co-Planar Electrodes in Microfluidic Chips. *AIP Adv* **2014**, *4*, 067103.
(9) Im, D. J. Next Generation Digital Microfluidic Technology: Electrophoresis of Charged Droplets. *Korean J. Chem. Eng.* **2015**, *32*, 1001−1008.
(10) Guo, F.; Ji, X.-H.; Liu, K.; He, R.-X.; Zhao, L.-B.; Guo, Z.-X.; Liu, W.; Guo, S.-S.; Zhao, X.-Z. Droplet Electric Separator Microfluidic Device for Cell Sorting. *Appl. Phys. Lett.* **2010**, *96*, 193701.
(11) Ahn, B.; Lee, K.; Panchapakesan, R.; Oh, K. W. On-Demand Electrostatic Droplet Charging and Sorting. *Biomicrofluidics* **2011**, *5*, 024113.
(12) Cartier, C. A.; Graybill, J. R.; Bishop, K. J. M. Electric Generation and Ratcheted Transport of Contact-Charged Drops. *Phys. Rev. E* **2017**, *96*, 043101.
(13) Zagnoni, M.; Le Lain, G.; Cooper, J. M. Electrocoalescence Mechanisms of Microdroplets Using Localized Electric Fields in Microfluidic Channels. *Langmuir* **2010**, *26*, 14443−14449.
(14) Thiam, A. R.; Bremond, N.; Bibette, J. Breaking of an Emulsion under an AC Electric Field. *Phys. Rev. Lett.* **2009**, *102*, 188304.
(15) Chong, Z. Z.; Tan, S. H.; Gañán-Calvo, A. M.; Tor, S. B.; Loh, N. H.; Nguyen, N.-T. Active Droplet Generation in Microfluidics. *Lab Chip* **2016**, *16*, 35−58.
(16) Clausell-Tormos, J.; Lieber, D.; Baret, J.-C.; El-Harrak, A.; Miller, O. J.; Frenz, L.; Blouwolff, J.; Humphry, K. J.; Köster, S.; Duan, H.; et al. Droplet-Based Microfluidic Platforms for the Encapsulation and Screening of Mammalian Cells and Multicellular Organisms. *Chem. Biol.* **2008**, *15*, 427−437.
(17) Im, D. J.; Jeong, S.-N.; Yoo, B. S.; Kim, B.; Kim, D.-P.; Jeong, W.-J.; Kang, I. S. Digital Microfluidic Approach for Efficient Electroporation with High Productivity: Transgene Expression of Microalgae without Cell Wall Removal. *Anal. Chem.* **2015**, *87*, 6592−6599.
(18) Lee, S.; Lee, S.; Hwang, H.; Hong, J.; Lee, S.; Lee, J.; Chae, Y.; Lee, T. Ultrafast Single-Droplet Bouncing Actuator with Electrostatic Force on Superhydrophobic Electrodes. *RSC Adv.* **2016**, *6*, 66729−66737.
(19) Zhang, Y.; Liu, Y.; Wang, X.; Shen, Y.; Ji, R.; Cai, B. Investigation of the Charging Characteristics of Micrometer Sized Droplets Based on Parallel Plate Capacitor Model. *Langmuir* **2013**, *29*, 1676−1682.
(20) Cartier, C. A.; Drews, A. M.; Bishop, K. J. M. Microfluidic Mixing of Nonpolar Liquids by Contact Charge Electrophoresis. *Lab Chip* **2014**, *14*, 4230−4236.
(21) Bishop, K. J. M.; Drews, A. M.; Cartier, C. A.; Pandey, S.; Dou, Y. Contact Charge Electrophoresis: Fundamentals and Microfluidic Applications. *Langmuir* **2018**, *34*, 6315−6327.
(22) Im, D. J.; Yoo, B. S.; Ahn, M. M.; Moon, D.; Kang, I. S. Digital Electrophoresis of Charged Droplets. *Anal. Chem.* **2013**, *85*, 4038−4044.
(23) Maxwell, J. C. *A Treatise on Electricity and Magnetism*; Cambridge University Press, 2010; Vol. *1*.
(24) Elton, E. S.; Tibrewala, Y.; Rosenberg, E. R.; Hamlin, B. S.; Ristenpart, W. D. Measurement of Charge Transfer to Aqueous Droplets in High Voltage Electric Fields. *Langmuir* **2017**, *33*, 13945−13954.
(25) Im, D. J.; Ahn, M. M.; Yoo, B. S.; Moon, D.; Lee, D. W.; Kang, I. S. Discrete Electrostatic Charge Transfer by the Electrophoresis of a Charged Droplet in a Dielectric Liquid. *Langmuir* **2012**, *28*, 11656−11661.
(26) Im, D. J.; Noh, J.; Moon, D.; Kang, I. S. Electrophoresis of a Charged Droplet in a Dielectric Liquid for Droplet Actuation. *Anal. Chem.* **2011**, *83*, 5168−5174.
(27) Elton, E. S.; Rosenberg, E. R.; Ristenpart, W. D. Crater Formation on Electrodes during Charge Transfer with Aqueous Droplets or Solid Particles. *Phys. Rev. Lett.* **2017**, *119*, 094502.
(28) Jung, Y.-M.; Oh, H.-C.; Kang, I. S. Electrical Charging of a Conducting Water Droplet in a Dielectric Fluid on the Electrode Surface. *J. Colloid Interface Sci.* **2008**, *322*, 617−623.
(29) Jalaal, M.; Khorshidi, B.; Esmaeilzadeh, E. An experimental study on the motion, deformation and electrical charging of water drops falling in oil in the presence of high voltage D.C. electric field. *Exp. Therm. Fluid Sci.* **2010**, *34*, 1498−1506.
(30) Elton, E. S.; Tibrewala, Y. V.; Ristenpart, W. D. Droplet Conductivity Strongly Influences Bump and Crater Formation on Electrodes during Charge Transfer. *Langmuir* **2018**, *34*, 7284−7293.
(31) Tobazéon, R. Electrohydrodynamic Behaviour of Single Spherical or Cylindrical Conducting Particles in an Insulating Liquid Subjected to a Uniform DC Field. *J. Phys. D: Appl. Phys.* **1996**, *29*, 2595−2608.
(32) Drews, A. M.; Kowalik, M.; Bishop, K. J. M. Charge and Force on a Conductive Sphere between Two Parallel Electrodes: A Stokesian Dynamics Approach. *J. Appl. Phys.* **2014**, *116*, 074903.
(33) Cho, A. Y. H. Contact Charging of Micron-Sized Particles in Intense Electric Fields. *J. Appl. Phys.* **1964**, *35*, 2561−2564.
(34) Knutson, C. R.; Edmond, K. V.; Tuominen, M. T.; Dinsmore, A. D. Shuttling of Charge by a Metallic Sphere in Viscous Oil. *J. Appl. Phys.* **2007**, *101*, 013706.
(35) Drews, A. M.; Cartier, C. A.; Bishop, K. J. M. Contact Charge Electrophoresis: Experiment and Theory. *Langmuir* **2015**, *31*, 3808−3814.
(36) Eslami, G.; Esmaeilzadeh, E.; Pérez, A. T. Modeling of Conductive Particle Motion in Viscous Medium Affected by an Electric Field Considering Particle-Electrode Interactions and Micro-discharge Phenomenon. *Phys. Fluids* **2016**, *28*, 107102.
(37) Gu, H.; Murade, C. U.; Duits, M. H. G.; Mugele, F. A Microfluidic Platform for On-Demand Formation and Merging of Microdroplets Using Electric Control. *Biomicrofluidics* **2011**, *5*, 011101.
(38) Ahn, M. M.; Im, D. J.; Kang, I. S. Geometric Characterization of Optimal Electrode Designs for Improved Droplet Charging and Actuation. *Analyst* **2013**, *138*, 7362−7368.
(39) Eow, J. S.; Ghadiri, M. Motion, Deformation and Break-up of Aqueous Drops in Oils under High Electric Field Strengths. *Chem. Eng. Process.* **2003**, *42*, 259−272.
(40) Yang, S. H.; Im, D. J. Electrostatic Origins of the Positive and Negative Charging Difference in the Contact Charge Electrophoresis of a Water Droplet. *Langmuir* **2017**, *33*, 13740−13748.
(41) de la Mora, J. F. The Fluid Dynamics of Taylor Cones. *Annu. Rev. Fluid Mech.* **2007**, *39*, 217−243.
(42) Pohl, H. A. *Dielectrophoresis*; Cambridge University Press, 1978.
(43) Hamlin, B. S.; Creasey, J. C.; Ristenpart, W. D. Electrically Tunable Partial Coalescence of Oppositely Charged Drops. *Phys. Rev. Lett.* **2012**, *109*, 094501.
(44) Ristenpart, W. D.; Bird, J. C.; Belmonte, A.; Dollar, F.; Stone, H. A. Non-Coalescence of Oppositely Charged Drops. *Nature* **2009**, *461*, 377−380.
(45) Millikan, R. A. On the Elementary Electrical Charge and the Avogadro Constant. *Phys. Rev.* **1913**, *2*, 109−143.

DOI: 10.1021/acs.langmuir.8b04254
Langmuir 2019, 35, 3937−3948

(46) Hadamard, J. S. Mouvement Permanent Lent d'une Sphere Liquide et Visqueuse Dans Un Liquide Visqueux. *C. R. Acad. Sci.* **1911**, *152*, 1735−1743.
(47) Rybczynski, W. Über Die Fortschreitende Bewegung Einer Flssigen Kugel in Einem Zhen Medium. *Bull. Acad. Sci. Cracovi, A* **1911**, 40−46.
(48) Sachs, L. *Applied Statistics: A Handbook of Techniques*, 2nd ed.; Springer Series in Statistics; Springer-Verlag: New York, 1984.
(49) Box, G. E. P.; Jenkins, G. *Time Series Analysis: Forecasting and Control*, 5th ed.; Holden Day, 1976.
(50) Bliss, C. I.; Fisher, R. A. Fitting the Negative Binomial Distribution to Biological Data. *Biometrics* **1953**, *9*, 176−200.
(51) Jain, G. C.; Consul, P. C. A Generalized Negative Binomial Distribution. *SIAM J. Appl. Math.* **1971**, *21*, 501−513.
(52) Gurland, J. Some Applications of the Negative Binomial and Other Contagious Distributions. *American Journal of Public Health and the Nations Health* **1959**, *49*, 1388−1399.
(53) Carter, E. M.; Potts, H. W. Predicting Length of Stay from an Electronic Patient Record System: A Primary Total Knee Replacement Example. *BMC Med. Inf. Decis. Making* **2014**, *14*, 26.
(54) Abdel-Aty, M. A.; Radwan, A. E. Modeling Traffic Accident Occurrence and Involvement. *Accident Analysis & Prevention* **2000**, *32*, 633−642.
(55) Taylor, G. Disintegration of Water Drops in Electric Fields. *Proc. R. Soc. London, Ser. A* **1964**, *280*, 383−397.
(56) Gu, W.; Heil, P. E.; Choi, H.; Kim, K. Generation of stable multi-jets by flow-limited field-injection electrostatic spraying and their control viaI-Vcharacteristics. *J. Phys. D: Appl. Phys.* **2010**, *43*, 492001.
(57) Martin, S.; Perea, A.; Garcia-Ybarra, P. L.; Castillo, J. L. Effect of the Collector Voltage on the Stability of the Cone-Jet Mode in Electrohydrodynamic Spraying. *J. Aerosol Sci.* **2012**, *46*, 53−63.
(58) Gu, W.; Singh, R.; Kim, K. Flow-Limited Field-Injection Electrostatic Spraying for Controlled Formation of Charged Multiple Jets of Precursor Solutions: Theory and Application. *Appl. Phys. Lett.* **2005**, *87*, 084107.
(59) Rayleigh, L. On the Equilibrium of Liquid Conducting Masses Charged with Electricity. *Philos. Mag. J. Sci.* **1882**, *14*, 184−186.
(60) Li, K.-Y.; Tu, H.; Ray, A. K. Charge Limits on Droplets during Evaporation. *Langmuir* **2005**, *21*, 3786−3794.
(61) Duft, D.; Achtzehn, T.; Müller, R.; Huber, B. A.; Leisner, T. Rayleigh jets from levitated microdroplets. *Nature* **2003**, *421*, 128.
(62) Janouš, J.; Čech, J.; Beránek, P.; Přibyl, M.; Šnita, D. AC Electric Sensing of Slug-Flow Properties with Exposed Gold Microelectrodes. *J. Micromech. Microeng.* **2014**, *24*, 015002.

DOI: 10.1021/acs.langmuir.8b04254
Langmuir 2019, 35, 3937−3948